Breadfruit (*Artocarpus altilis)* contains some promising inhibitors of the M^{pro} enzyme of SARS-CoV-2: an *in silico* molecular docking and pharmacological analysis

Md Afif Ullah[1], Md Mehedy Hasan Miraz[1], Nilay Saha[1], Arghya Prosun Sarkar[2], Bidduth Kumar Sarkar[3] and Sukalyan Kumar Kundu[1,*]

[1]*Department of Pharmacy, Jahangirnagar University, Savar, Dhaka-1342, Bangladesh*

[2]*Department of Pharmacy, Faculty of Biological Sciences, Islamic University, Kushtia, Bangladesh*

[3]*Department of Pharmacy, Faculty of Science, Comilla University, Cumilla*

*** Corresponding Author**
Sukalyan Kumar Kundu
Department of Pharmacy, Jahangirnagar University
Savar, Dhaka, Bangladesh.
Email: skkbd415@juniv.edu
Phone: +8801731291468

Abstract

The world experienced a sudden outbreak of an abruptly emerging virus, SARS-CoV-2, in late December 2019 in the city of Wuhan, China. Within a few months, the resulting disease, COVID-19, had taken over a major portion of the world. Researchers have since been working with the viral targets, aiming to unwrap an absolute cure. Because of the severity and concerns about the virus, we conducted a computational assessment of compounds derived from breadfruit (*Artocarpus altilis*) to study. The assessment aims to unveil some promising compounds as inhibitors of SARS-CoV-2. We selected the main protease (M^{pro}) enzyme of SARS-CoV-2, since this enzyme is responsible for the replication process of the virus. Initially we had gone for a drug-likeness analysis to screen the most suitable compounds. Afterwards, molecular dockings were performed with the selected compounds from *A. altilis*. Nirmatrelvir was taken as a standard inhibitor in this study, as it is an FDA approved drug in combination with ritonavir. In molecular docking, the test compounds, cycloartomunin, dihydrocycloartomunin, cycloartobiloxanthone, artomunoxanthentrione, and cycloartomunoxanthone exhibited binding affinities of −7.6, −7.7, −7.7, −8.3, and −8.1 kcal/mol, respectively. Nirmatrelvir showed an affinity of −8.1 kcal/mol while docking on the same server. Consequently, a pharmacological analysis was conducted with the top five test compounds compared with the standard inhibitor. A computational toxicity analysis was also involved in this assessment. Finally, the test compounds were found to have promising docking outputs, and moderate pharmacological profiles. After all, this study scrutinized the test compounds and suggests further validations to confirm the potentiality of the compounds inhibiting the SARS-CoV-2 M^{pro} enzyme.

Keywords: COVID-19, SARS-CoV-2, mpro, breadfruit, *Artocarpus altilis*, molecular docking.

1. Introduction

The SARS-CoV-2 outbreak in late 2019 and its global propagation have had substantial global consequences on public health, economics, and social aspects (Miyah et al., 2022). SARS-CoV-2, also known as COVID-19, is a highly pathogenic virus that was discovered in Wuhan, China, near the end of 2019. Since then, it has swiftly spread over the world, and the World Health Organization (WHO) designated it a global pandemic in March 2020 (Patnaik, 2021). As a result of the pandemic, many countries throughout the world imposed tight measures such as lockdowns and travel restrictions to prevent the spread of COVID-19 (Inoue & Todo, 2020; Zhong et al., 2021). Until April 15, 2023, the World Health Organization (WHO) had recorded over 762 million COVID-19 cases globally (https://covid19.who.int/). Regrettably, the aforementioned has led to a total of more than 6.84 million fatalities, which is a substantial figure in comparison to other diseases (WHO, 2023).

The causative agent of COVID-19, SARS-CoV-2, is a positive-sense, single-stranded RNA virus belonging to the family of Coronaviridae (Hu et al., 2020). The virus has a unique spike protein on its surface that binds to the human angiotensin-converting enzyme 2 (ACE2) receptor, facilitating its entry into host cells and subsequent replication (Deng et al., 2021). The SARS-CoV-2 virus has undergone significant mutations, leading to the emergence of several new variants (WHO, 2022).

Among the proteins of SARS-CoV-2, the main protease (M^{pro}) enzyme plays a critical role in viral replication and is considered a promising drug target for therapeutic intervention against COVID-19 (Huynh et al., 2021). M^{pro}, also known as 3CL pro, is responsible for the proteolytic cleavage of the viral polypeptide during replication, which is essential for the production of functional viral proteins (Dharmashekara et al., 2021). The inhibition of M^{pro} can potentially prevent viral replication and transmission, making it a valuable target for drug development against COVID-19. The structural and functional characteristics of M^{pro} have been extensively studied in recent times, leading to the development of several inhibitors targeting this protease. These inhibitors have shown effective inhibition of M^{pro} in vitro and in vivo, demonstrating their potential as a therapeutic option for treating COVID-19 (Li et al., 2021).

Artocarpus altilis, commonly referred to as breadfruit, belongs to the family Moraceae. It is a notable plant with a substantial therapeutic profile (Sikarwar et al., 2014). Many ongoing studies are looking at the pharmacological effects of Artocarpus altilis. Anti-inflammatory activity, antifungal potential, sexual behavior study, immunomodulatory potential, anti-diabetic activity, antibacterial activity, anti-cholinergic effect, chelating activity, nutritional assessment, as a cosmetic agent, ACE inhibitors, and other studies are being conducted on these plants. Surprisingly, the activity of this plant against SARS-CoV-2 was previously undocumented in the literature. As a result, it was chosen for this investigation to investigate its action against the targets of Omicron variant SARS-CoV-2.

Nirmatrelvir–ritonavir (Paxlovid™), which has received Emergency Use Authorization by the Food and Drug Administration (FDA) for the outpatient treatment of COVID-19 infection in adults (Gui et al., 2023). Nirmatrelvir is a SARS-CoV-2 M^{pro} inhibitor, which actively inhibits the viral replication process by blocking the virus from cleaving viral polyproteins into their functional parts, thus limiting the infection's spread in the body (Park et al., 2022). Multiple studies have shown that nirmatrelvir–ritonavir has potent inhibitory activity against SARS-CoV-2 proteases, making it a promising candidate for COVID-19 treatment (Rodrigues et al., 2022). A clinical trial by Pfizer, the developer of nirmatrelvir/ritonavir, reported that nirmatrelvir/ritonavir treatment reduced the risk of hospitalization or death by 89% in patients with mild to moderate COVID-19 symptoms (Huang et al., 2022). Thus, we have considered nirmatrelvir as a standard inhibitor in our assessment.

Computer-aided drug design (CADD) is a computational method that uses various software tools and algorithms to create, optimize, and test new drugs before they can be synthesized and tested in the lab (Yu & MacKerell, 2017). In this computational assessment, we implemented molecular docking, pharmacokinetic and pharmacodynamic property studies to discover the best possible drug candidate. Molecular docking provided us with information on each ligand's binding affinity, direction, and kind of interaction with the appropriate target proteins. The pharmacokinetic profiles were obtained in order to analyze data on the absorption, distribution, metabolism, and excretion (ADME) of chemicals that occur inside the body following medication delivery. To determine the LD50 values and toxicity classes of the various ligands, a toxicology scrutiny was conducted.

In the current work, we used a screening method to filter out 10 phytochemical compounds from *A. altilis* based on drug-likeness criteria. Through preliminary computational analysis, the compounds were examined across a wide spectrum of studies. As a result, this framework evaluates and offers potential promising *A. altilis* medication candidates against the SARSCoV-2 Omicron B.1.1.529 strain.

2. Materials and Methods

2.1. Selection and Preparation of Ligands

A total of ten phytochemicals derived from *Artocarpus altilis* were chosen for this investigation based on their drug-likeness. The molecules were chosen using Lipinski's rule of five and Ghose filter (Ghose et al., 1999; Lipinski et al., 1997). Only molecules that followed both rules were chosen for this investigation. The chosen ligands' 3D conformers were obtained in SDF format from the online databases PubChem (https://pubchem.ncbi.nlm.nih.gov/) and IMPPAT 2.0 (Indian Medicinal Plants, Phytochemistry, and Therapeutics; https://cb.imsc.res.in/imppat/) (Kim et al., 2016; Vivek-Ananth et al., 2023).

2.2. Retrieval and Preparation of Target Protein

The crystal structure of the M^{pro} enzyme (PDB ID: 8D4L) of SARS-CoV-2 was retrieved in PDB format from the RCSB Protein Data Bank database (https://www.rcsb.org/) (Dejnirattisai et al., 2022; Rose et al., 2016). The resolution of the downloaded spike protein was 1.70°A. The protein structures were cleaned by eliminating unwanted atoms and molecules (including ligands) with PyMOL version 2.5.2 software (Schrodinger, LLC) (Lill et al., 2011). The receptor-binding domain (RBD) of the spike protein was extracted from the crystal structure, and the superfluous chains of proteins were eliminated using PyMOL. The proteins' chains were stored in PDB formats for molecular docking.

2.3. Molecular Docking

The CB-Dock2 server (https://cadd.labshare.cn/cb-dock2/php) was used to execute molecular dockings on the chosen ligands against the target proteins (Liu et al., 2022). The binding affinity (kcal/mol) for each protein-ligand combination, as well as noncovalent interactions and docking orientations, were examined using the Dassault Systmes BIOVIA Discovery Studio 2021 Client version 21.1.0 software. The 2D and 3D schematic drawings of the protein-ligand docking complexes were obtained from BIOVIA Discovery Studio.

2.4. ADME and Toxicity Prediction

The top-docking ligands' canonical SMILES were taken from the PubChem and IMPPAT 2.0 databases and entered into the SwissADME website (https://www.swissadme.ch/) (Daina et al., 2017).

SwissADME provided the ADME (absorption, distribution, metabolism, and excretion) statistics for each ligand. Following that, the ProTox-II service (https://tox-new.charite.de/protox_II/) was used to estimate the toxicity profile of each ligand (Banerjee et al., 2018). These two sources were used to record the physicochemical, pharmacokinetic, and pharmacodynamic aspects of each ligand. During the ADME and toxicity prediction, each ligand's topological polar surface area (TPSA), lipophilicity (MLogP), water solubility (LogS), bioavailability score, blood-brain barrier (BBB) permeability, interaction with P-glycoprotein (P-gp), LD50 value, and toxicity class were explored.

3. Results and Discussion

The docking score or binding affinity of a ligand denotes the level of attraction at which the ligand is supposed to bind to the target. The docking conformations shows at which orientation the ligands bind to the respective targets. A complete docking operation includes the bond types, bond lengths, and a complete overview on the ligands static interactions with the target. Artomunoxanthentrione displayed the highest binding affinity, that is −8.3 kcal/mol. It was found to exhibit almost 20 interactions with the amino acid residues of M^{pro}. The interactions obtained from the CB-Dock2 server for each molecule has been mentioned in table 1. the binding affinities of cycloartomunin, cihydrocycloartomunin, cycloartobiloxanthone, artomunoxanthentrione, cycloartomunoxanthone, and nirmatrelvir (standard) in complex were −7.6, −7.7 , −7.7, −8.1, and −8.1 kcal/mol, respectively. Figure 1 depicts a graphically comparative overview of the docking scores (binding affinities) of all test compounds and the standard inhibitor. A diagrammatic scheme of the types of 3D conformations (obtained from CB-Dock2 server) and 2D interactions (obtained from BIOVIA Discovery Studio software) have been shown in Figure 2.

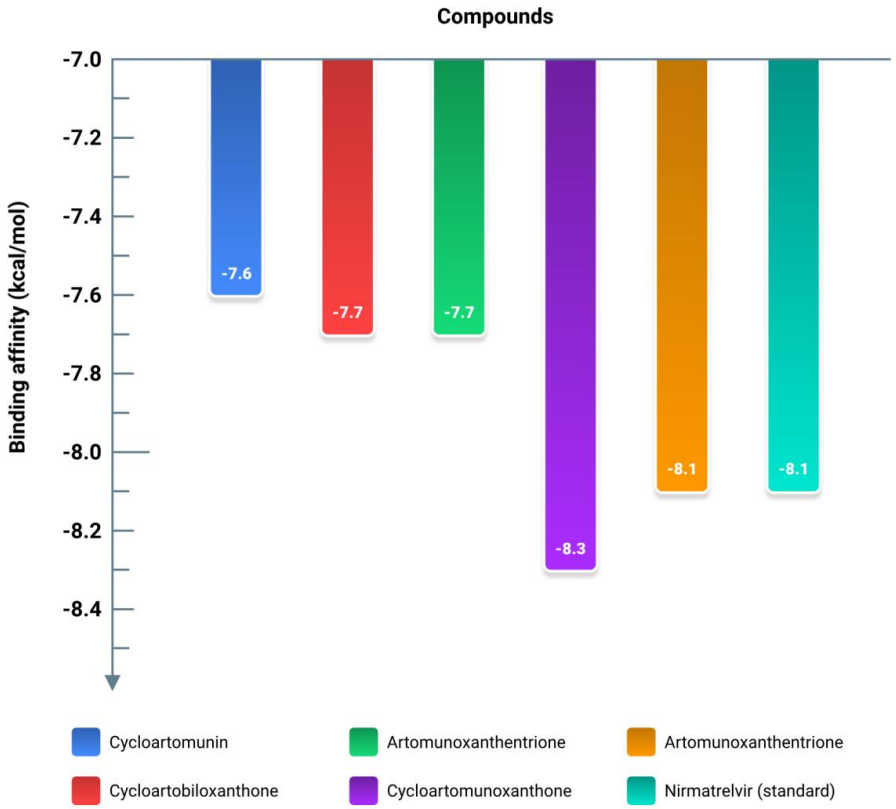

Figure 1: Binding affinity chart of each compound in complex with M^{pro} enzyme of SARS-CoV-2.

Table 1: The binding affinities and noncovalent (hydrogen bonds and hydrophobic) interactions of the test compounds and the standard inhibitor (nirmatrelvir).

Chemical ID (Source)	Compound Name	Binding affinity (kcal/mol)	Interactions
IMPHY000132 (IMPPAT)	Cycloartomunin	−7.6	GLN107 PRO108 GLY109 GLN110 PRO132 ILE200 VAL202 GLU240 PRO241 HIS246 ILE249 THR292 PRO293 PHE294
IMPHY000674 (IMPPAT)	Dihydrocycloartomunin	−7.7	THR24 THR25 THR26 LEU27 HIS41 CYS44 THR45 SER46 MET49 PHE140 LEU141 ASN142 GLY143 ALA144 CYS145 HIS163 HIS164 GLU166 HIS172 GLN189
IMPHY001232 (IMPPAT)	Cycloartobiloxanthone	−7.7	HIS41 MET49 LEU141 ASN142 GLY143 CYS145 HIS163 HIS164 MET165 GLU166 LEU167 PRO168 GLN189
IMPHY001629 (IMPPAT)	Artomunoxanthentrione	−8.3	THR24 THR25 THR26 LEU27 HIS41 CYS44 THR45 SER46 MET49 PHE140 LEU141 ASN142 GLY143 ALA144 CYS145 HIS163 GLU166 LEU167 PRO168 GLN189
IMPHY001678 (IMPPAT)	Cycloartomunoxanthone	−8.1	THR24 THR25 THR26 HIS41 CYS44 THR45 SER46 MET49 PHE140 LEU141 ASN142 GLY143 ALA144 CYS145 HIS163 HIS164 MET165 GLU166 HIS172 GLN189
155903259 (PubChem)	Nirmatrelvir	−8.1	THR25 THR26 LEU27 HIS41 CYS44 THR45 SER46 MET49 PHE140 LEU141 ASN142 GLY143 ALA144 CYS145 HIS163 HIS164 MET165 GLU166 ARG188 GLN189

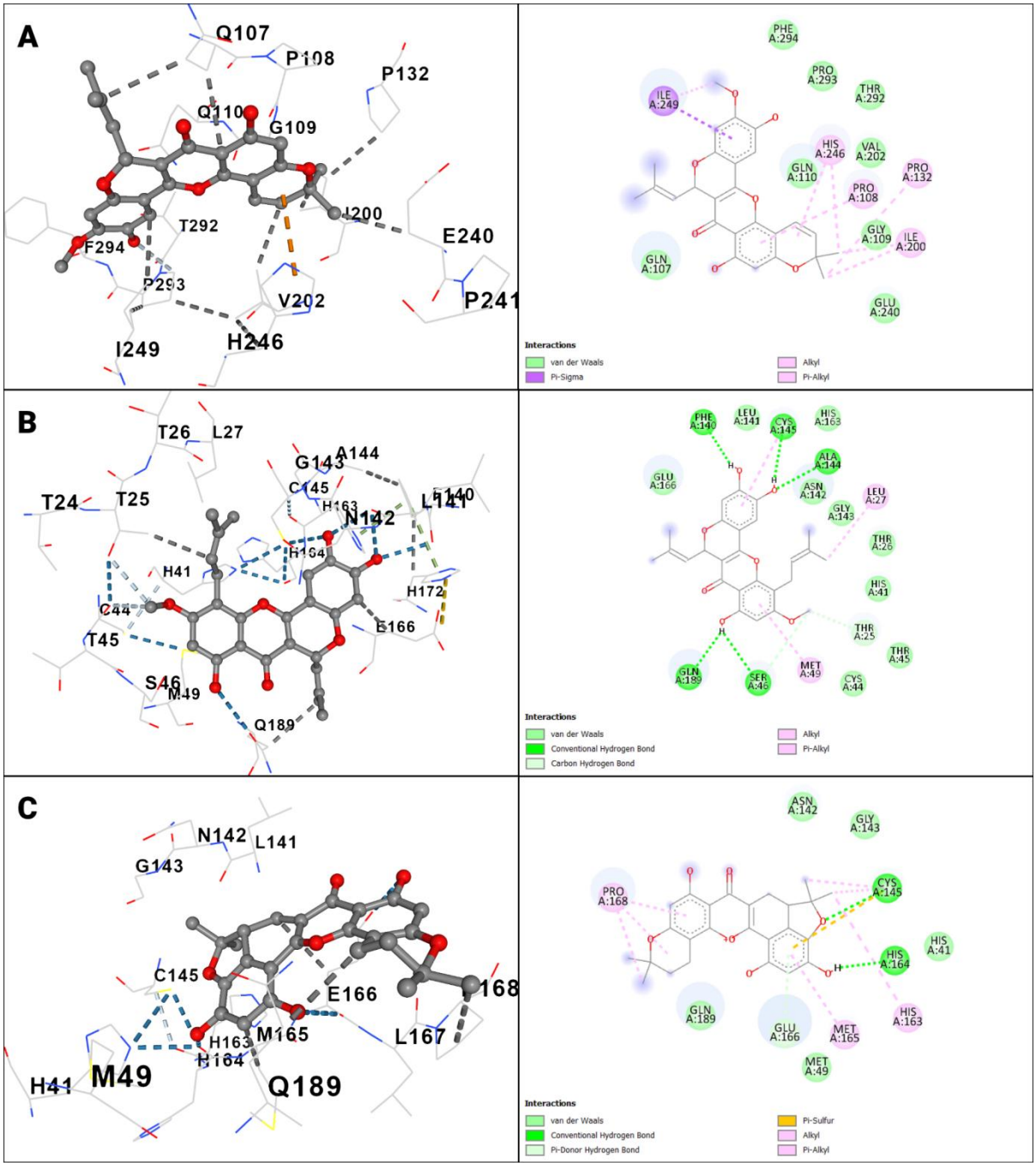

Figure 2: 3D conformations (left) and 2D view of the docking outputs of (A) cycloartomunin, (B) dihydrocycloartomunin, (C) cycloartobiloxanthone, (D) artomunoxanthentrione, (E) cycloartomunoxanthone, and (F) nirmatrelvir in complex with M^{pro}.

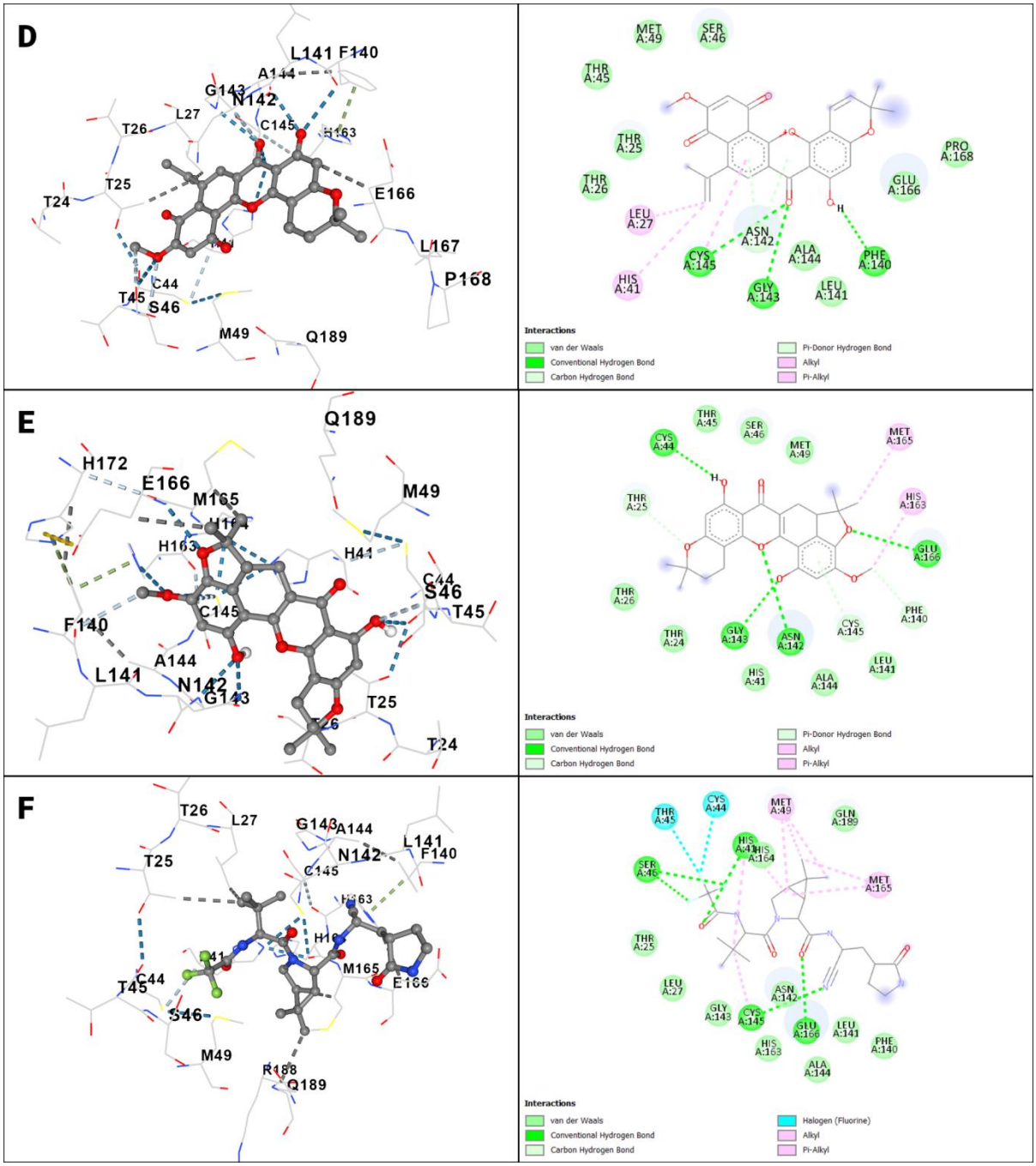

Figure 2: (continued).

The physicochemical, pharmacokinetic, and pharmacodynamic aspects of the compounds were analyzed using the data obtained from Protox-II and SwissADME. The ADME profiles give a detailed overview of the molecular weights (MWs), topological polar surface areas (TPSAs), lipophilicity, water solubility, gastrointestinal absorptions, bioavailability scores, blood-brain barrier (BBB) permeability, and certain parameters for the ligands. These factors reflect how well molecules will be absorbed, distributed, metabolized, and eventually eliminated once they reach the human body. All of the molecules under investigation have been found to conform to Lipinski's rule of five and the Ghose rule, indicating their potential for oral bioavailability.

In particular, the relationship between the TPSA value and the permeability of the blood-brain barrier has been considered, with TPSA below 90 $Å^2$ being associated with higher permeability and those above 140 $Å^2$ being linked to lower permeability (Hitchcock & Pennington, 2006; Pajouhesh & Lenz, 2005). Among the test compounds, cycloartomunoxanthone exhibits the lowest TPSA of 96.36 $Å^2$, while dihydrocycloartomunin and cycloartobiloxanthone shows the highest TPSA, that is 109.36 $Å^2$. However, artomunoxanthentrione and cycloartomunin showed TPSA values of 103.04 $Å^2$ and 98.36 $Å^2$, respectively. Normatrelvir, the standard inhibitor exhibits a TPSA of 131.40 $Å^2$.

According to Lipinski's rule of five, drugs intended for oral administration should have a lipophilicity value below 5.0. All molecules investigated in this study were found to have lipophilicity (MLogP) below this threshold. Artomunoxanthentrione exhibited the lowest MLogP value as a test compound, which is 1.06, whereas that of cycloartomunoxanthone is 1.84 (highest among the test compounds). Cycloartomunin, dihydrocycloartomunin, and cycloartobiloxanthone have MLogP values of 1.77, 1.77, and 1.63, respectively (as shown in Table 2). The standard inhibitor, nirmatrelvir, has a value of 0.41. Water solubility (LogS (ESOL)) was also investigated for each compound. Cycloartomunin, dihydrocycloartomunin, cycloartobiloxanthone, artomunoxanthentrione, and cycloartomunoxanthone have LogS (ESOL) values of −6.10, −6.39, −5.46, −6.05, and −5.67, respectively. Nirmatrelvir occupies a LogS (ESOL) of −3.58. All five of the test compounds were found to have poor water solubility except cycloartobiloxanthone and cycloartomunoxanthone (both are moderately soluble). However, all the test compounds and the standard inhibitor show high gastrointestinal absorption, and each has a bioavailability score of 0.55, except artomunoxanthentrione (0.56). Cycloartobiloxanthone and Cycloartomunoxanthone were found to be substrates of the P-glycoprotein (P-gp).

In terms of toxicity, the lethal dose 50 (LD50) for cycloartomunin, dihydrocycloartomunin, cycloartobiloxanthone, artomunoxanthentrione, and cycloartomunoxanthone are 5000, 5000, 2500, 120, and 5000 mg/kg, respectively. All test compounds except artomunoxanthentrione belong to toxicity class 5. The toxicity class of artomunoxanthentrione is 3. Nirmatrelvir, on the other hand, has a LD50 of 3000 mg/kg and belongs to toxicity class 5. It is important to mention that the higher the toxicity class, the safer the molecule would be while considering the amount administered.

Table 2: The physicochemical, pharmacokinetic, and pharmacodynamic properties of the molecules with the top 6 docking scores retrieved from SwissADME and Protox-II.

Property	Cycloartomunin	Dihydrocycloartomunin	Cycloartobiloxanthone	Artomunoxanthentrione	Cycloartomunoxanthone	Nirmatrelvir (standard)
MW (g/mol)	448.46	450.48	434.44	444.43	448.46	499.53
TPSA (Å²)	98.36	109.36	109.36	103.04	96.36	131.40
MLogP	1.77	1.77	1.63	1.06	1.84	0.41
LogS (ESOL)	−6.10	−6.39	−5.46	−6.05	−5.67	−3.58
ESOL Class	Poorly soluble	Poorly soluble	Moderately soluble	Poorly soluble	Moderately soluble	Soluble
GI absorption	High	High	High	High	High	High
Bioavailability score	0.55	0.55	0.55	0.56	0.55	0.55
BBB permeant	No	No	No	No	No	No
P-gp substrate	No	No	Yes	No	Yes	Yes
Lipinski's RO5 vio.	0	0	0	0	0	0
Ghose filter vio.	0	0	0	0	0	0
LD50 (mg/kg)	5000	5000	2500	120	5000	3000
Toxicity class	5	5	5	3	5	5

MW: molecular weight; TPSA: topological polar surface area; MLogP: lipophilicity; LogS (ESOL): water solubility; ESOL class: water solubility class; GI absorption: gastrointestinal absorption; bioavailability score: Abbott bioavailability score; BBB permeant: blood-brain barrier permeability; P-gp substrate: interaction with P-glycoprotein; Lipinski Vio: number of violations of Lipinski's rule of Gve; Ghose Vio: number of violations of Ghose's rule; LD50 (mg/kg):lethal dose 50; toxicity class: class based on LD50 value.

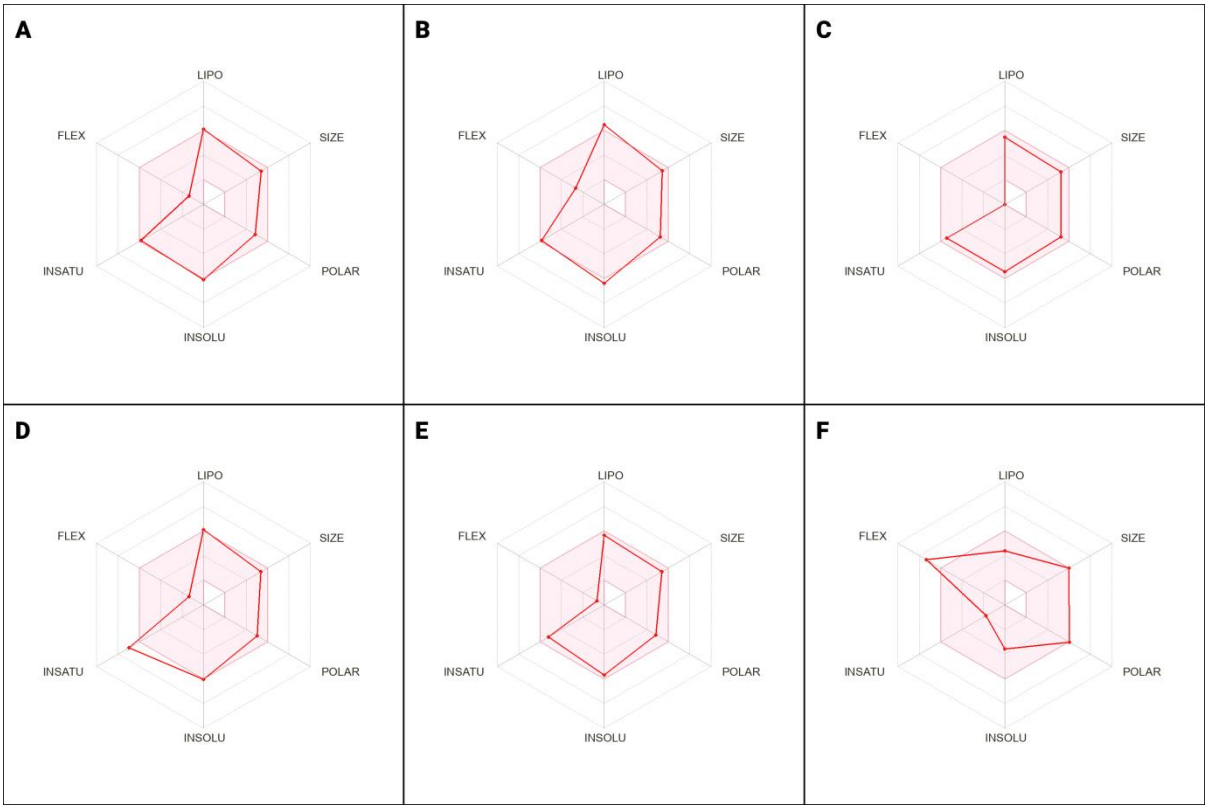

Figure 3: The bioavailability radars of (A) cycloartomunin, (B) dihydrocycloartomunin, (C) cycloartobiloxanthone, (D) artomunoxanthentrione, (E) cycloartomunoxanthone, and (F) nirmatrelvir retrieved from SwissADME. The colored zone is the suitable physicochemical space for oral bioavailability. LIPO (Lipophilicity): −0.7 < XLOGP3 < +5.0; SIZE: 150g/mol < MV < 500g/mol; POLAR (Polarity): 20Å² < TPSA < 130Å²; INSOLU (Insolubility): −6 < Log S (ESOL) < 0; INSATU (Insaturation): 0.25 < Fraction Csp3 < 1; FLEX (Flexibility): 0 < Num. rotatable bonds < 9.

4. Conclusion

The goal of this study was to look at compelling compounds from breadfruit (*Artocarpus altilis)* in order to trace possible inhibitors of the M^{pro} enzyme of SARS-CoV-2. Artomunoxanthentrione and cycloartomunoxanthone were found to have affinities above and equal to the standard inhibitor. Artomunoxanthentrione had the highest binding affinity when docked with the target. Moreover, cycloartomunin, dihydrocycloartomunin, and cycloartobiloxanthone also displayed good interactions with the target. This study, however, solely investigates the in silico characteristics and profiles of the phytochemicals from *Artocarpus altilis*. Additional validations are demanded to confirm the efficacy and potentiality of the test compounds as potential inhibitors of the SARS-CoV-2 target enzyme. As a result of this, our study's findings suggest cycloartomunin, dihydrocycloartomunin, cycloartobiloxanthone, artomunoxanthentrione, and cycloartomunoxanthone as promising candidates against the M^{pro} enzyme of SARS-CoV-2.

[Continued in the next page.]

Conflicts of Interest

The authors declare no conflicts of interest.

Acknowledgments

Earnest gratitude to Dr. Sukalyan Kumar Kundu, Professor of Pharmacy for his role in providing the facilities and his contribution to conducting this study successfully.

Attachments

Figures: Go to the following link to download high resolutions of the figures: https://drive.google.com/drive/folders/1qZN5BscDg2dfCHeBAWseGvOnv0FQsWYG?usp=sharing

---

References

Banerjee, P., Eckert, A. O., Schrey, A. K., & Preissner, R. (2018). ProTox-II: A webserver for the prediction of toxicity of chemicals. *Nucleic Acids Research*, *46*(W1), Article W1. https://doi.org/10.1093/nar/gky318

Daina, A., Michielin, O., & Zoete, V. (2017). SwissADME: A free web tool to evaluate pharmacokinetics, drug-likeness and medicinal chemistry friendliness of small molecules. *Scientific Reports*, *7*(1), Article 1. https://doi.org/10.1038/srep42717

Dejnirattisai, W., Huo, J., Zhou, D., Zahradník, J., Supasa, P., Liu, C., Duyvesteyn, H. M. E., Ginn, H. M., Mentzer, A. J., Tuekprakhon, A., Nutalai, R., Wang, B., Dijokaite, A., Khan, S., Avinoam, O., Bahar, M., Skelly, D., Adele, S., Johnson, S. A., … Young, P. (2022). SARS-CoV-2 Omicron-B.1.1.529 leads to widespread escape from neutralizing antibody responses. *Cell*, *185*(3), Article 3. https://doi.org/10.1016/j.cell.2021.12.046

Deng, Q., Rasool, R. ur, Russell, R. M., Natesan, R., & Asangani, I. A. (2021). Targeting androgen regulation of TMPRSS2 and ACE2 as a therapeutic strategy to combat COVID-19. *IScience*, *24*(3), Article 3. https://doi.org/10.1016/j.isci.2021.102254

Dharmashekara, C., Pradeep, S., Prasad, S. K., Jain, A. S., Syed, A., Prasad, K. S., Patil, S. S., Beelagi, M. S., Srinivasa, C., & Shivamallu, C. (2021). Virtual screening of potential phyto-candidates as therapeutic leads against SARS-CoV-2 infection. *Environmental Challenges*, *4*, 100136. https://doi.org/10.1016/j.envc.2021.100136

Ghose, A. K., Viswanadhan, V. N., & Wendoloski, J. J. (1999). A Knowledge-Based Approach in Designing Combinatorial or Medicinal Chemistry Libraries for Drug Discovery. 1. A Qualitative and Quantitative Characterization of Known Drug Databases. *Journal of Combinatorial Chemistry*, *1*(1), Article 1. https://doi.org/10.1021/cc9800071

Guex, N., & Peitsch, M. C. (1997). SWISS-MODEL and the Swiss-Pdb Viewer: An environment for comparative protein modeling. *Electrophoresis*, *18*(15), Article 15. https://doi.org/10.1002/elps.1150181505

Gui, H., Zhang, Z., Chen, B., Chen, Y., Wang, Y., Long, Z., Zhu, C., Wang, Y., Cao, Z., & Xie, Q. (2023). Development and validation of a nomogram to predict failure of 14-day negative nucleic acid conversion

in adults with non-severe COVID-19 during the Omicron surge: A retrospective multicenter study. *Infectious Diseases of Poverty*, *12*(1), 7. https://doi.org/10.1186/s40249-023-01057-4

Hitchcock, S. A., & Pennington, L. D. (2006). Structure−Brain Exposure Relationships. *Journal of Medicinal Chemistry*, *49*(26), Article 26. https://doi.org/10.1021/jm060642i

Hu, B., Guo, H., Zhou, P., & Shi, Z.-L. (2021). Characteristics of SARS-CoV-2 and COVID-19. *Nature Reviews Microbiology*, *19*(3), Article 3. https://doi.org/10.1038/s41579-020-00459-7

Huang, J., Yin, D., Qin, X., Yu, M., Jiang, B., Chen, J., Cao, Q., & Tang, Z. (2022). Case report: Application of nirmatrelvir/ritonavir to treat COVID-19 in a severe aplastic anemia child after allogeneic hematopoietic stem cell transplantation. *Frontiers in Pediatrics*, *10*, 935118. https://doi.org/10.3389/fped.2022.935118

Huynh, T., Cornell, W., & Luan, B. (2021). In silico Exploration of Inhibitors for SARS-CoV-2's Papain-Like Protease. *Frontiers in Chemistry*, *8*, 624163. https://doi.org/10.3389/fchem.2020.624163

Inoue, H., & Todo, Y. (2020). The propagation of economic impacts through supply chains: The case of a mega-city lockdown to prevent the spread of COVID-19. *PLOS ONE*, *15*(9), Article 9. https://doi.org/10.1371/journal.pone.0239251

Kim, S., Thiessen, P. A., Bolton, E. E., Chen, J., Fu, G., Gindulyte, A., Han, L., He, J., He, S., Shoemaker, B. A., Wang, J., Yu, B., Zhang, J., & Bryant, S. H. (2016). PubChem Substance and Compound databases. *Nucleic Acids Research*, *44*(D1), D1202–D1213. https://doi.org/10.1093/nar/gkv951

Li, Q., Wu, J., Nie, J., Zhang, L., Hao, H., Liu, S., Zhao, C., Zhang, Q., Liu, H., Nie, L., Qin, H., Wang, M., Lu, Q., Li, X., Sun, Q., Liu, J., Zhang, L., Li, X., Huang, W., & Wang, Y. (2020). The Impact of Mutations in SARS-CoV-2 Spike on Viral Infectivity and Antigenicity. *Cell*, *182*(5), Article 5. https://doi.org/10.1016/j.cell.2020.07.012

Li, X., Lidsky, P. V., Xiao, Y., Wu, C.-T., Garcia-Knight, M., Yang, J., Nakayama, T., Nayak, J. V., Jackson, P. K., Andino, R., & Shu, X. (2021). Ethacridine inhibits SARS-CoV-2 by inactivating viral particles. *PLOS Pathogens*, *17*(9), Article 9. https://doi.org/10.1371/journal.ppat.1009898

Lill, M. A., & Danielson, M. L. (2011). Computer-aided drug design platform using PyMOL. *Journal of Computer-Aided Molecular Design*, *25*(1), Article 1. https://doi.org/10.1007/s10822-010-9395-8

Lipinski, C. A., Lombardo, F., Dominy, B. W., & Feeney, P. J. (2001). Experimental and computational approaches to estimate solubility and permeability in drug discovery and development settings 1PII of original article: S0169-409X(96)00423-1. The article was originally published in Advanced Drug Delivery Reviews 23 (1997) 3–25. 1. *Advanced Drug Delivery Reviews*, *46*(1–3), Article 1–3. https://doi.org/10.1016/S0169-409X(00)00129-0

Liu, Y., Yang, X., Gan, J., Chen, S., Xiao, Z.-X., & Cao, Y. (2022). CB-Dock2: Improved protein–ligand blind docking by integrating cavity detection, docking and homologous template fitting. *Nucleic Acids Research*, *50*(W1), Article W1. https://doi.org/10.1093/nar/gkac394

Maycock, A. L., Abeles, R. H., Salach, J. I., & Singer, T. P. (1976). The structure of the covalent adduct formed by the interaction of 3-dimethylamino-1-propyne and the flavine of mitochondrial amine oxidase. *Biochemistry*, *15*(1), Article 1. https://doi.org/10.1021/bi00646a018

Miyah, Y., Benjelloun, M., Lairini, S., & Lahrichi, A. (2022). COVID-19 Impact on Public Health, Environment, Human Psychology, Global Socioeconomy, and Education. *The Scientific World Journal*, *2022*, 1–8. https://doi.org/10.1155/2022/5578284

Rose, P. W., Prlić, A., Altunkaya, A., Bi, C., Bradley, A. R., Christie, C. H., Costanzo, L. D., Duarte, J. M., Dutta, S., Feng, Z., Green, R. K., Goodsell, D. S., Hudson, B., Kalro, T., Lowe, R., Peisach, E., Randle, C., Rose, A. S., Shao, C., … Burley, S. K. (2017). The RCSB protein data bank: Integrative view of protein, gene and 3D structural information. *Nucleic Acids Research*, *45*(D1), D271–D281. https://doi.org/10.1093/nar/gkw1000

Pajouhesh, H., & Lenz, G. R. (2005). Medicinal chemical properties of successful central nervous system drugs. *NeuroRX*, *2*(4), Article 4. https://doi.org/10.1602/neurorx.2.4.541

Park, J. J., Lee, J., Seo, Y. B., & Na, S. H. (2022). Nirmatrelvir/Ritonavir Prescription Rate and Outcomes in Coronavirus Disease 2019: A Single Center Study. *Infection & Chemotherapy*, *54*(4), 757. https://doi.org/10.3947/ic.2022.0123

Patnaik, U. J. 2. (2021). Review article on COVID-19 and Guillain-Barré syndrome. *Frontiers in Bioscience-Scholar*, *13*(1), Article 1. https://doi.org/10.52586/S555

Rodrigues, L., Bento Cunha, R., Vassilevskaia, T., Viveiros, M., & Cunha, C. (2022). Drug Repurposing for COVID-19: A Review and a Novel Strategy to Identify New Targets and Potential Drug Candidates. *Molecules*, *27*(9), 2723. https://doi.org/10.3390/molecules27092723

Sikarwar, M. S., Hui, B. J., Subramaniam, K., Valeisamy, B. D., Yean, L. K., & Balaji, K. (2014). A Review on Artocarpus altilis (Parkinson) Fosberg (breadfruit). *Journal of Applied Pharmaceutical Science*, *4*(8), 091–097. https://doi.org/10.7324/JAPS.2014.40818

Vivek-Ananth, R. P., Mohanraj, K., Sahoo, A. K., & Samal, A. (2023). IMPPAT 2.0: An Enhanced and Expanded Phytochemical Atlas of Indian Medicinal Plants. *ACS Omega*, *8*(9), 8827–8845. https://doi.org/10.1021/acsomega.3c00156

Yu, W., & MacKerell, A. D. (2017). Computer-Aided Drug Design Methods. In P. Sass (Ed.), *Antibiotics* (Vol. 1520, pp. 85–106). Springer New York. https://doi.org/10.1007/978-1-4939-6634-9_5

Zhong, L., Diagne, M., Wang, W., & Gao, J. (2021). Country distancing increase reveals the effectiveness of travel restrictions in stopping COVID-19 transmission. *Communications Physics*, *4*(1), Article 1. https://doi.org/10.1038/s42005-021-00620-5